Proceedings of the 21st ICSMGE, Vienna, Austria, 14 – 19 June 2026. Pistrol, Adam & Schweiger (eds.)
Published by: ÖGG, Austrian Society for Geomechanics, Salzburg, Austria, ISBN 978-3-9503898-4-5
https://doi.org/10.53243/ICSMGE2026-31

Seismic Interaction between three adjacent buildings on liquefiable soils

Yu-Wei Hwang, Cheng-Hsu Yang, Lee-Yi Wang, Ying-Hsuan Chen, Louis Ge
Department of Civil Engineering, National Taiwan University, Taiwan, yuweihwang@ntu.edu.tw

ABSTRACT: The resilience of a city after an extreme event, like an earthquake, depends on the resilience of various infrastructure and buildings. In particular, after the 2022 Chishang Earthquake, the Central Weather Bureau stated that large-scale earthquakes are very likely to occur in western Taiwan in the future since the accumulation of seismic energy in this area has not been released so far. Hence, the design and damage assessment of existing or new infrastructure and buildings on liquefiable sites near active faults are critical issues for geotechnical engineers in Taiwan. A series of centrifuge experiments were first conducted to understand the structure-soil-structure interactions for three adjacent 5-story buildings (SSSI) on liquefiable soils under pulse-like motion, as compared to the case of a single 5-story building (representing SSI). The experimental results showed that the mid-building under SSSI experienced much less foundation tilt as compared to the corner building or isolated building. Meanwhile, a notable permanent foundation tilt was observed for the corner building at the end of the earthquake shaking. Subsequently, a limited numerical sensitivity study was performed to explore the impact of building spacing, velocity impulse, and ground motion intensity on SSSI and SSI via using finite element analyses, OpenSees. In general, the numerical results showed that the building(s) under pulse-like motion experienced greater foundation settlements and tilts as compared to those under non-pulse-like motions. On the other hand, greater foundation tilts but less foundation settlements were observed for buildings at shorter spacings, particularly for the corner buildings. The experimental and numerical results highlight the significance of considering the effects of SSSI and velocity impulse on building performance. There is an urgent need for improved guidelines when assessing and addressing liquefaction in urban environments.

KEYWORDS: Structure-soil-structure interaction, soil liquefaction, pulse-like motion, finite element analysis, centrifuge experiment

1 INTRODUCTION

Soil liquefaction during earthquakes has caused extensive infrastructure damage in seismic events such as the 2016 Meinong earthquake (Tsai et al. 2018) and the 2023 Kahramanmaraş earthquake in Turkey (Moug et al., 2024). Although research has thoroughly examined isolated buildings on liquefiable soils (Allmond and Kutter, 2012; Olarte et al., 2017), urban environments typically feature closely spaced structures with complex interactions. Recent studies investigating structure-soil-structure interaction (SSSI) between neighboring buildings have identified key mechanisms affecting seismic performance: alteration of static stress fields, changes in inertial demand, and kinematic constraints imposed by adjacent foundations (Kirkwood and Dashti, 2018a,b). Research indicates that building spacing, structural properties, soil permeability (Qi and Knappett, 2022), and the characteristics of liquefiable layers significantly influence settlement and tilting patterns (Hwang et al., 2021). A cluster of three aligned structures is considered the most critical configuration when evaluating SSSI effects because of its notable static stress field bias beneath the foundations. Ground motion characteristics also play a vital role, with pulse-like motions potentially increasing liquefaction risk (Green et al., 2008; Dong et al., 2018). While the interaction between two nearby structures has received attention, the behavior of three or more buildings remains largely unexplored (Hwang and Dashti, 2023). This study employed a series of three-dimensional finite element analyses to assess how building properties, spacing, and ground motion characteristics influence key engineering demand parameters.

2 CENTRIFUGE TESTING PROGRAM

Wang (2025) conducted centrifuge experiments at National Central University to evaluate SSI and SSSI on layered, liquefiable ground. Test layouts included TB_{SSI} (one isolated tall building) and $TB_{SSSI\text{-}S5}$ (three aligned tall buildings with 5m edge-to-edge spacing), as shown in Figure 1a. All experimental results are presented in prototype scale. The soil profile consisted of a 13m-thick dense layer of quartz sand (Dr≈80%) beneath a 5m-thick loose sand layer (Dr≈50%) with groundwater at surface level. Structure TB represented a 5-story aluminum frame structure on a 1m-thick mat foundation, with 17m total height. The foundation footprint size was 5m×5m, and the embedment depth was about 1 m. The foundation bearing pressure was approximately 130 kPa, with a static factor of safety of about 1.5. A methylcellulose solution with a viscosity 65 times that of water was used as the pore fluid during specimen saturation. Subsequently, a series of one-dimensional (1D) horizontal earthquake motions was applied, after each model was spun to a nominal centrifugal acceleration of 65 g at the center of the loose sand layer. The experimental results from the first major motion, referred to as ChiChi-P, were obtained from the 1999 Chi-Chi earthquake at the TCU052 station. These results were used to validate the numerical framework. The peak ground acceleration (PGA) of the ChiChi-P motion was 0.22g. Figure 1b illustrates the acceleration time history and the 5%-damped acceleration response spectrum of the ChiChi-P motion, recorded at the base of the container during tests.

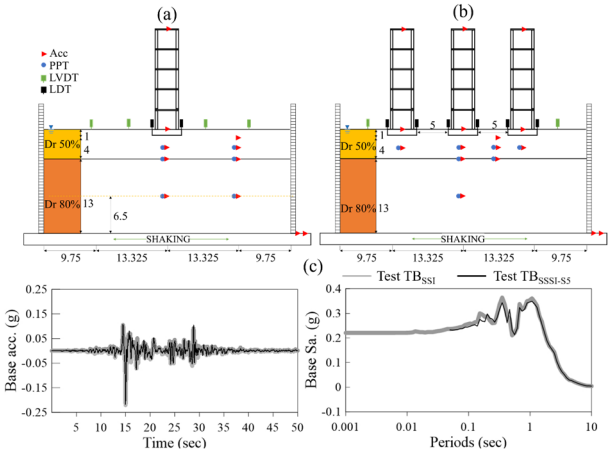

Figure 1. (a) Test layout of Models TB_{SSI} and $TB_{SSSI\text{-}S5}$ in the centrifuge experiments in elevation view; (b) Time history and response spectrum (5%-damped) of the base acceleration recorded during the first major event, ChiChi-P.

3 NUMERICAL MODELLING OF SOIL-FOUNDATION-STRUCTURE SYSTEMS

3.1 *Three-dimensional numerical framework*

Three-dimensional (3D) numerical simulations were conducted using a parallel version of the object-oriented, open-source finite element framework, OpenSEESMP. Figure 2 displays a schematic representation of a numerical model that investigates structure-soil-structure interaction.

Soil was modeled using 8-node brick elements with the u-p formulation (Zienkiewicz et al. 1990). The fluid bulk modulus was taken as 2×10^6 kPa. To account for the reduction in the soil's shear modulus caused by liquefaction, the mesh size was set as 0.5 m in elevation. The cyclic response of saturated, granular soils was simulated using the pressure-dependent, multi-yield surface 03 constitutive model PDMY03 (Khosravifar et al. 2018). In this study, soil parameters were calibrated based on two key factors: (1) the experimental results from a series of direct shear tests and (2) the centrifuge test conducted on an isolated tall building (TB_{SSI}), which was founded on the same soil profile illustrated in Fig. 1a. Table 1 shows the calibrated PDMY03 parameters. A Rayleigh damping ratio of 3% was used to dissipate seismic energy at small strains.

The foundation was modeled as a linear-elastic material using SSPbrick elements. The foundation elements were connected to the surrounding soil elements through an equal-degree-of-freedom connection along the perimeter of the foundation. The nodes at the perimeter were only linked to the adjacent soil nodes in the horizontal direction, while the bottom of the foundation elements was fully connected to the soil elements. The structure's beams and columns were modeled with elastic beam-column elements and a linear elastic material. Inertial masses and gravity loads were applied at each floor level of the superstructure.

Periodic boundary conditions were applied in all numerical simulations. To enhance computational efficiency, only half of the model was simulated in the direction perpendicular to the shaking, based on the assumption of model symmetry, as shown in Fig. 2. Out-of-plane displacements (perpendicular to shaking) were restricted at the symmetry face and its parallel counterpart. All nodes at the base and sides of the soil domain were set as impervious boundaries. The soil's bottom boundary was fixed in all directions, simulating a rigid container base in the centrifuge. The recorded acceleration time history at the base of the container during the ChiChi-P motion (Fig. 1b) was directly applied to the base nodes after the soil-foundation-structure system achieved initial gravity equilibrium.

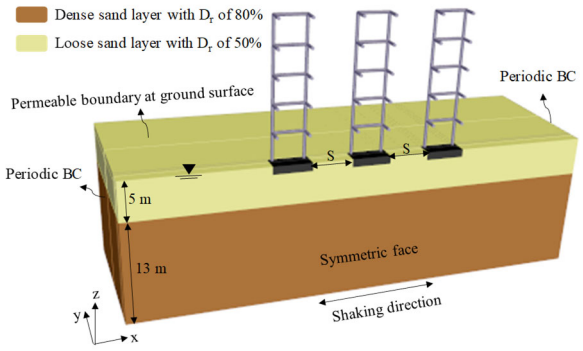

Figure 2. Schematic drawing of the numerical model for Model TB_{SSSI}.

Table 1. Calibrated soil parameters for the PDMY03 model.

Description		
Relative density, D_r (%)	50	80
Saturated unit weight, γ_{sat} (kN/m^3)	19.05	19.89
Reference effective confining pressure, P'_r (kPa)	101	101
Pressure dependence coefficient, d	0.5	0.5
Reference small-strain shear modulus, $G_{max,ref}$ (MPa)	82	105
Friction angle, ϕ' (°)	27	37
Phase transformation angle, ϕ_{pt} (°)	24.5	32.5
Contraction coefficients, c_a, c_b, c_c, c_d, and c_e	0.12 6.0 0.3 12.5 1	0.027 0.5 0.55 4.6 -0.5
Dilation coefficients, d_a, d_b, and d_c	0.2 3.0 -0.25	0.38 3.0 -0.463
Hydraulic conductivity, *k* (m/s)	1.41×10^{-4}	1.19×10^{-4}

3.2 *Model Validation*

Figure 3 compares experimental and numerical results for Models TB_{SSI} and $TB_{SSSI\text{-}S5}$, focusing specifically on foundation settlement and tilt responses. The numerical framework showed acceptable accuracy in capturing these foundation behaviors, with computational predictions closely matching experimental measurements along the 1:1 correspondence line. In Model $TB_{SSSI\text{-}S5}$, the middle building showed minimal rotational response, while the left building exhibited significantly greater foundation tilt, exceeding even that of the isolated building in Model TB_{SSI}. The numerical model accurately predicted the average foundation settlement for each building in both cases. Experimental measurements and numerical simulations both demonstrated that buildings under SSSI experienced less foundation settlement compared to those under SSI. Although sensor signal loss occurred for both settlement and tilt measurements of the right building in $TB_{SSSI\text{-}S5}$, the consistent agreement observed for the left and middle buildings confirmed the robustness of the numerical approach in capturing settlement and tilt patterns of building clusters on liquefiable ground.

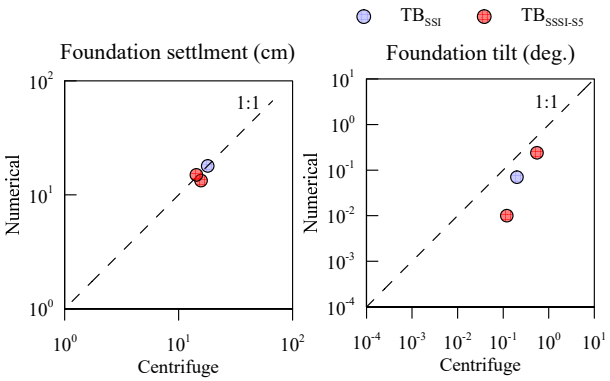

Figure 3. Comparison of centrifuge experimental and numerical results for models TB_{SSI} and $TB_{SSSI\text{-}S5}$.

4 DESIGN OF NUMERICAL SENSITIVITY STUDY

A numerical sensitivity study was performed to investigate the key trends in how SSSI and ground motion characteristics influence the performance of buildings with shallow foundations on liquefiable soils. The building clusters consisted of three structures with foundation edge-to-edge spacings (S) of 1.25, 2.5, 5, and 10 m. The notation used for different models

first identifies whether the building experienced SSI or SSSI. The second subscript indicated the edge-to-edge spacings (S). On the other hand, the influence of ground motion characteristics on seismic interactions was evaluated by considering the pulse-like (P) and non-pulse-like (NP) characteristics, while keeping other parameters the same. Two ground motions were selected from the NGA West2 database (https://ngawest2.berkeley.edu/). The pulse-like motion was selected based on rupture distance less than 10 km and with pulse characteristics identified from the NGA West2 database. For NP motions, horizontal component pairs were rotated to determine the maximum rotated peak ground acceleration (RotD100). Alternatively, P motion components were rotated to identify the direction of maximum velocity, which was then used as the 1D input motion for the 3D numerical simulations. The 1989 Loma Prieta earthquake (RSN:810) was selected as the NP motion with PGA of 0.45g and cumulative absolute velocity (CAV) of 1265 cm/s. Similarly, the 2010 Darfield earthquake (RSN:6911) represented the selected P motion with similar PGA of 0.44g and similar CAV of 1488 cm/s. Figure 4 shows the acceleration time histories and 5%-damped spectral accelerations of the selected motions. In conclusion, a total of 40 numerical models were considered in this study. All the influencing parameters were carefully selected to clearly show whether the influencing parameter would bring a positive or negative impact on the engineering demand parameters (EDPs) of interest.

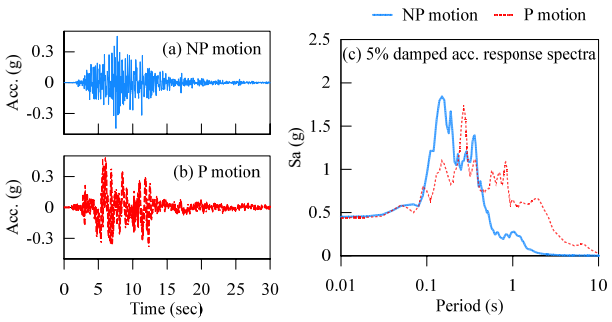

Figure 4. Time history and 5%-damped acceleration response spectra of the ground motions in numerical sensitivity study.

5 NUMERICAL RESULTS

5.1 *Soil response at near field*

Figures 5 and 6 present the settlement contours and shear strain (γ_{xz}) distributions for building clusters with spacings of 1.25 m and 10 m, respectively, under different ground motion characteristics. For the closely spaced configuration (S = 1.25 m), the settlement patterns under NP motion showed substantially increased settlements developing beneath all three buildings, forming a unified subsidence zone. This settlement pattern indicated significant interaction among the closely spaced buildings during intense shaking, effectively behaving as a single wider foundation system. When subjected to P motion, despite similar PGA values, the distinct velocity pulse characteristics (PGV = 99.7 cm/s compared to 17.8 cm/s for NP) notably changed the settlement distribution, creating more pronounced differential settlement and significantly greater tilt tendencies, particularly for the side buildings.

For the widely spaced configuration (S = 10 m), buildings under NP motion maintained relatively distinct subsidence zones, indicating reduced structure-soil-structure interaction at larger spacings despite the high intensity. However, when subjected to P motion, the velocity pulse encouraged deeper and more asymmetric settlement patterns. For conditions considered, this demonstrated that pulse-like motion might amplify SSSI effects even at larger distances between structures, overcoming the isolation typically observed at wider spacings.

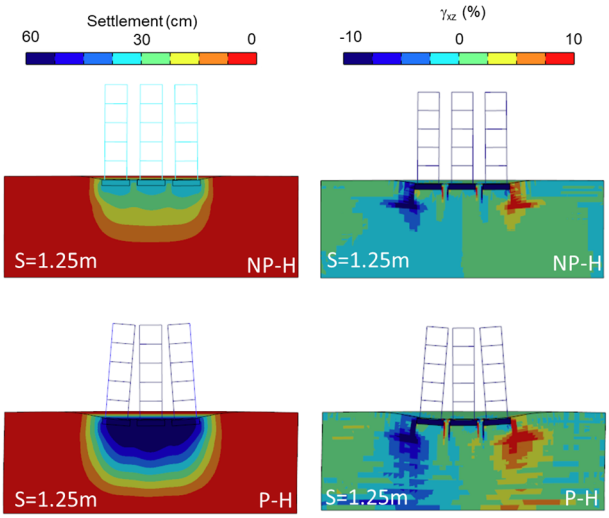

Figure 5. The settlement contours and shear strain distributions for tall building clusters with a spacing of 1.25 m under different ground motions.

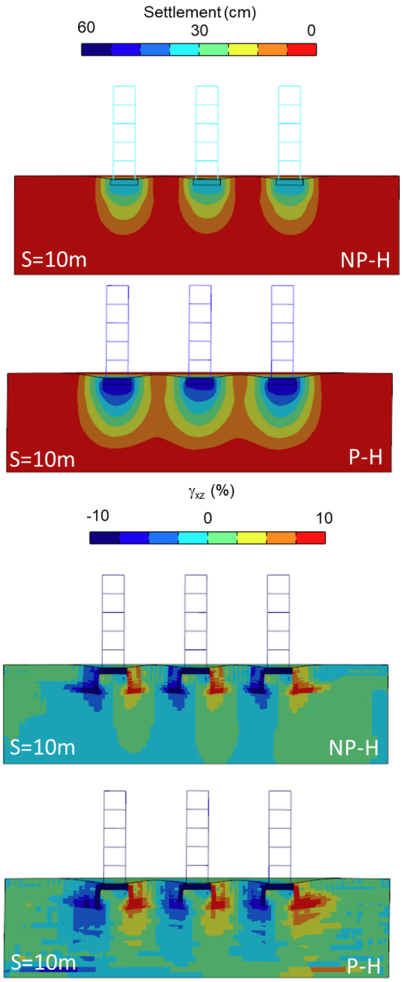

Figure 6. The settlement contours and shear strain distributions for tall building clusters with a spacing of 10 m under different ground motions.

The shear strain (γ_{xz}) distributions provided additional insight into the deformation mechanisms influenced by pulse

characteristics. For the closely spaced cluster under NP motion, the shear strain distribution became highly asymmetric and intense beneath all foundations, leading to greater differential settlements and rotational tendencies. However, P motion led to even more severe and concentrated shear strain patterns, with extreme values particularly beneath the side buildings. The directivity effects and strong velocity pulse in P motion created highly localized strain concentrations that substantially increased rotational demands compared to the more evenly distributed pattern under NP motion.

For conditions considered, in general, the pulse-like characteristics of P motion not only increased the magnitude of settlement and shear deformation but also generated substantially more asymmetric responses and greater differential movements compared to NP motion with similar PGA. These effects highlight the critical importance of considering not only the intensity but also the pulse characteristics of ground motions when evaluating SSSI in urban environments.

5.2 *Foundation and superstructure response*

Figures 7 and 8 present the key engineering demand parameters (EDPs) for side buildings and middle buildings in Models TB_{SSSI} under NP and P motions, respectively. For permanent foundation settlement, buildings under NP motion experienced approximately 31 cm of settlement across all three structures, while P motion significantly increased the settlement to about 60 cm, roughly double the amount observed under NP-H. This substantial difference highlights the significant impact of pulse characteristics on liquefaction-induced settlement. Unlike NP case where settlement under SSSI showed minimal deviation from SSI (variations typically less than 10%), the foundation settlement under P motion demonstrated greater sensitivity to SSSI effects, with variations of up to 60-70% at closer spacings ($S \leq 2.5$ m), particularly for the middle building. This suggests that for pulse-like motions, seismic coupling more significantly influences settlement response, especially at shorter building spacings.

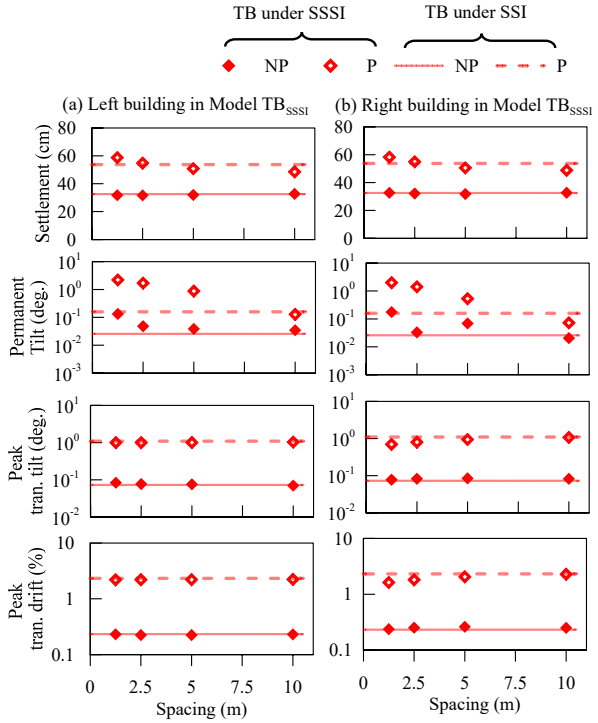

Figure 7. Key engineering demand parameters for Model TB_{SSI} and side buildings in Model TB_{SSSI} under different ground motions and building spacings.

For the conditions considered, the permanent tilt response revealed important differences between NP and P motions. For edge buildings under NP motion, permanent foundation tilt was notably reduced at $S < 10$ m, while P motion consistently encouraged significantly greater permanent tilt than NP motion across all spacings. For the case under P motion, although the absolute tilt magnitudes were considerably larger, the SSSI-induced tilt amplification (by about 4-6 times compared to SSI) followed similar trends as observed for NP motion, with edge buildings showing greater sensitivity to spacing than the middle building.

Peak transient foundation tilt remained around 0.07° for edge buildings under NP motion, while under P motion, these values increased significantly to nearly 1.0°. This large difference shows the strong effect of velocity pulses on rotational demands. For the peak transient drift ratio, P motions caused drift ratios almost 8 times larger than NP motions across all buildings, emphasizing the severe impact of pulse characteristics on foundation demands.

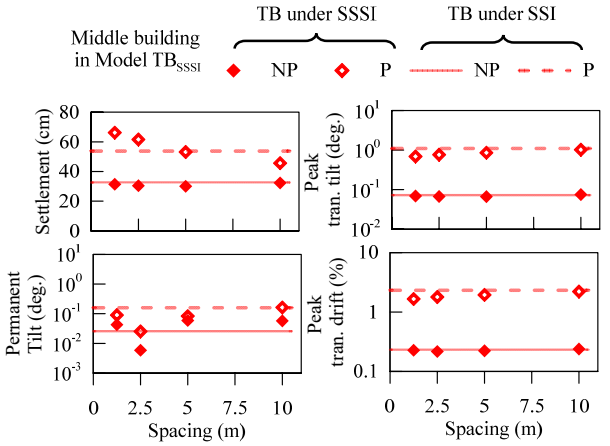

Figure 8. Key engineering demand parameters for Models TB_{SSI} and middle building in Model TB_{SSSI} under different ground motions and building spacings.

Figure 9 shows the tilt time histories of the three buildings in Models TB_{SSSI} with different building spacings. A clear difference in rotational behavior was observed between NP and P motions. Under NP motion, the outer buildings initially rotated inward during the first 10 seconds of strong shaking, then switched to outward rotation for the rest of the motion. This change in rotational behavior helped reduce the permanent tilt of the outer buildings by partially offsetting the initial inward rotation. In contrast, for aligned buildings under P motion, the edge buildings experienced noticeable rotational excursions almost immediately after the velocity pulse arrived. Unlike the slow phase change observed in NP cases, the P-H motion showed more continuous rotation in the same direction over time, leading to much larger permanent tilts. The middle building generally showed a greater rotational response under P motion compared to NP, though still less than the edge buildings.

Figure 10 illustrates the effective horizontal stress profile near the inner and outer edges of the edge buildings in Model $TB_{SSSI\text{-}S1.25}$ under various ground motions, as a representative example. For NP motion, the difference in lateral stress between the soil column near the inner and outer foundation edges was minor compared to P motion. The velocity pulse in P motion increased the degree and extent of excess pore water buildup, which contributed to soil softening both in the near field and far field. This resulted in a greater accumulation of soil deformations between foundations due to increased out-of-plane shear stress concentration, especially when the spacing

between foundations was shorter. This led to a strong inward rotation tendency for side structures under P motion, contrasting with the phase transition behavior observed under NP motion.

In summary, the comparisons between NP and P motions highlight the profound influence of pulse characteristics on foundation response. The velocity pulse in P motion not only amplified settlement magnitudes and dramatically increased tilt and drift demands compared to NP motion but also affected the patterns of building rotation and structure-soil-structure interaction. While both motions showed sensitivity to building spacing, with rotational interactions becoming negligible as spacing increased to 10 m, the P motion consistently produced more severe and permanent deformations across all engineering demand parameters, emphasizing the critical importance of considering pulse characteristics in seismic design for building clusters in near-fault regions.

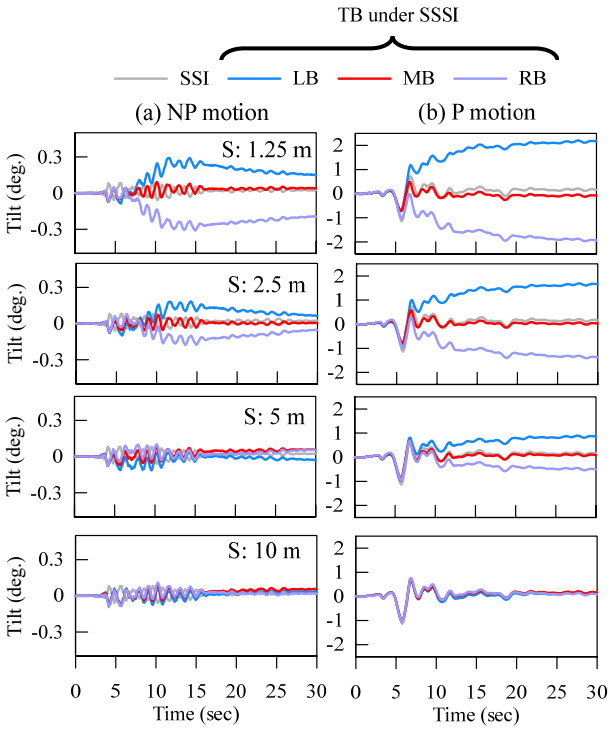

Figure 9. The tilt time histories of the three buildings in Models TB_{SSSI} under various ground motions and building spacings, comparing the left building (LB), middle building (MB), and right building (RB) responses.

6 CONCLUSIONS

This paper investigated the seismic interaction of three aligned structures on liquefiable soils through 3D nonlinear finite-element analyses, exploring the effects of building spacing, ground motion characteristics, and building properties on key engineering demand parameters.

Structure-soil-structure interaction (SSSI) effects were most significant at smaller spacings and diminished beyond S ≈ 10 m. Middle buildings experienced different seismic demands compared to edge buildings due to symmetric confinement, resulting in minimal tilt, while edge buildings often experienced amplified permanent tilt. Ground motion characteristics greatly influenced SSSI effects. Pulse-like motions caused significantly more settlements (about twice as much as non-pulse-like motion) and greatly increased tilt responses. Additionally, under NP motion, edge buildings initially rotated inward before transitioning to outward rotation, reducing permanent tilt by counteracting the initial rotation.

For the conditions considered, these findings generally highlight the importance of considering SSSI when evaluating liquefaction consequences in urban environments. Further research is needed to explore more complex urban configurations and develop mitigation strategies that account for SSSI effects, such as optimized ground improvement layouts for building clusters rather than individual structures.

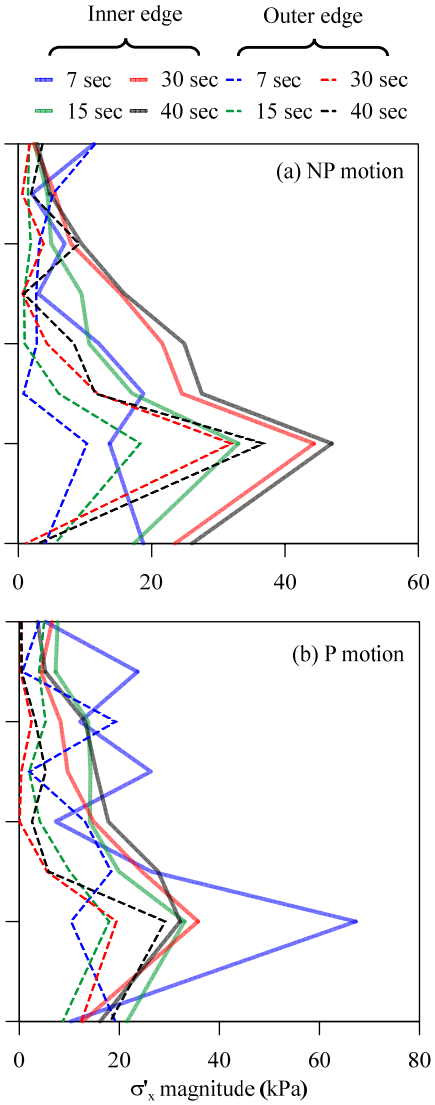

Figure 10. The effective horizontal stress profile near the inner and outer edges of the edge buildings in Models $TB_{SSSI\text{-}S1.25}$ at different time slots under different ground motions.

7 ACKNOWLEDGEMENTS

This study is supported by the National Science and Technology Council of Taiwan under Grant No. 114-2625-M-002 -019 -.

8 REFERENCES

Allmond, J. and Kutter, B.L., 2012. Centrifuge testing of rocking foundations on saturated sand and unconnected piles: The fluid response. In Proc., GeoCongress 2012: State of the Art and Practice in Geotechnical Engineering, pp.1760--1769. Reston, VA: ASCE.

Dong, W., Gao, G., Chen, J. and Jian, S., 2018. Effects of near-fault pulse-like ground motion on site liquefaction and settlement. In: Qiu, T., Tiwari, B., Zhang, Z. (eds) Proceedings of GeoShanghai 2018 International Conference: Advances in Soil Dynamics and Foundation Engineering. GSIC 2018. Springer, Singapore.

Green, R.A., Lee, J., White, T.M. and Baker, J.W., 2008. The significance of near-fault effects on liquefaction. In Proc., 14th World Conference on Earthquake Engineering. Tokyo: International Association for Earthquake Engineering.

Hwang, Y.W. and Dashti, S., 2023. Seismic interactions among multiple structures founded on liquefiable soils in a city block. Journal of Geotechnical and Geoenvironmental Engineering, 149(9), p.04023077.

Hwang, Y., Ramirez, J., Dashti, S., Kirkwood, P., Liel, A.B., Camata, G. and Petracca, M., 2021. Seismic interaction of adjacent structures on liquefiable soils: insight from centrifuge and numerical modeling. Journal of Geotechnical and Geoenvironmental Engineering, 147(8), p.04021063.

Khosravifar, A., Elgamal, A., Lu, J. and Li, J., 2018. A 3D model for earthquake-induced liquefaction triggering and post-liquefaction response. Soil Dynamics and Earthquake Engineering, 110, pp.43-52.

Kirkwood, P. and Dashti, S., 2018a. A centrifuge study of seismic structure-soil-structure interaction on liquefiable ground and the implications for structural performance. Earthquake Spectra, 34(3), pp.1113--1134.

Kirkwood, P. and Dashti, S., 2018b. Considerations for mitigation of earthquake-induced soil liquefaction in urban environments. Journal of Geotechnical and Geoenvironmental Engineering, 144(10), p.04018069.

Moug, D.M., Bray, J.D., Bassal, P. et al., 2024. Liquefaction-induced ground and building interactions in İskenderun from the 2023 Kahramanmaraş earthquake sequence. Earthquake Spectra, 40(2), pp.913-938.

Olarte, J., Paramasivam, B., Dashti, S., Liel, A. and Zannin, J., 2017. Centrifuge modeling of mitigation-soil-foundation-structure interaction on liquefiable ground. Soil Dynamics and Earthquake Engineering, 97, pp.304--323.

Qi, S. and Knappett, J.A., 2021. Effect of soil permeability on soil--structure and structure--soil--structure interaction of low-rise structures. Géotechnique, 72(9), pp.784--799.

Tsai, C.C., Hsu, S.Y., Wang, K.L., Yang, H.C., Chang, W.K., Chen, C.H. and Hwang, Y.W., 2018. Geotechnical reconnaissance of the 2016 ML6. 6 Meinong earthquake in Taiwan. Journal of Earthquake Engineering, 22(9), pp.1710-1736.

Wang, L.Y., 2025. Seismic interaction of three adjacent structures on liquefiable soil. Master's degree dissertation, National Yang Ming Chiao Tung University.

Zienkiewicz, O.C., Chan, A.H.C., Pastor, M., Paul, D.K. and Shiomi, T., 1990. Static and dynamic behaviour of soils: A rational approach to quantitative solutions. I: Fully saturated problems. In Proc., Royal Society of London, Series A, Mathematical and Physical Sciences, pp.285--309. London: Royal Society Publishing.